This manuscript is a preprint and has not been peer reviewed. The copyright holder has made the manuscript available under a Creative Commons Attribution 4.0 International (CC BY) license and consented to have it forwarded to EarthArXiv for public posting.

Meteorological Drought Magnitude, Duration, and Intensity in the Past and Future Climate of Eastern Tigray, Northern Ethiopia

Damasco Rubangakene[1,2*], Gloria Peace Lamaro[1',3], Stephen Komakech[4], Atkilt Girma[1,5&], Amanuel Zenebe[1,5&]

[1] Institute of Climate and Society, Mekelle University, P. O. Box 231, Mekelle, Ethiopia.

[2] Department of Geography, Faculty of Education, Gulu University, P.O. Box 166, Gulu

[3] College of Dryland Agriculture and Natural Resources, Mekelle University. P.O. Box 231, Mekelle, Ethiopia

[4] Uganda National Meteorological Authority, Kampala, P.O. Box: 7025, Kampala, Uganda

[5] Department of Land Resources Management and Environmental Protection (LaRMEP). Mekelle University, P.O. Box 231, Mekelle, Ethiopia

E-Mail: D.R. (aduudamasco@gmail.com); A.G. (atkiltg@gmail.com); A.Z. (zenebe@mu.edu.et); G.P.L. (peaceglam@gmail.com); S.K. (kstevostephen@gmail.com)

*** Corresponding author**

Email: aduudamasco@gmail.com (D.R.)

[&]These authors also contributed equally to this work.

This manuscript is a preprint and has not been peer reviewed. The copyright holder has made the manuscript available under a Creative Commons Attribution 4.0 International (CC BY) license and consented to have it forwarded to EarthArXiv for public posting.

ABSTRACT

Drought assessment is a critical component of risk management in the comprehensive analysis of drought impacts. This study assessed the meteorological drought events under the past and future climate of Eastern Tigray, Northern Ethiopia, with the principal objective of enhancing early warnings and better drought disaster response mechanisms. To predict future climate, delta scenarios were created from 20 GCMs CMIP5, and Bias corrected Spatially Downscaled dataset. GCM ensembles were used to analyze the 4- and 12-month Standardized Precipitation Index (SPI) and Standardized Precipitation and Evapotranspiration Index (SPEI). The SPI and SPEI indices were computed using the two-parameter gamma probability (α, β) and log-logistic distributions (α, β and γ), respectively. The two indices revealed historical drought years 1982-83, 1984, 1985, 1999, 2002, 2003, 2004, 2005, 2008 and 2009. Based on the predicted climate data, SPI and SPEI indices revealed that Atsbi will likely experience a higher total magnitude of both short-term and long-term drought under the future climate. Considering short-term drought, the total number of consecutive dry months is expected to increase more in Fatsi based on both the SPEI-4 and SPI-4 timescales. Wukro, on the other hand, will experience the greatest increase in consecutive dry months in all-time segments and emission scenarios. Although the predicted climate shows increased precipitation in the future, it's characteristically intermittent wet-dry cycles, coupled with higher evapotranspiration due to higher temperatures. We recommend the adoption of climate-resilient rainwater harvesting and water conservation agriculture.

Keywords: Global Circulation Model, Climate Change, Drought, Representative Concentration Pathways, SPI, SPEI.

This manuscript is a preprint and has not been peer reviewed. The copyright holder has made the manuscript available under a Creative Commons Attribution 4.0 International (CC BY) license and consented to have it forwarded to EarthArXiv for public posting.

1. Introduction

Drought is a life-threatening natural peril with extensive impacts, including soil damage, livelihood, economic losses and health (1). Globally, more than 2 billion people are affected by drought alone, yet a lot more than 11 million have died since 1900 as a result of drought (FAO, 2012). Ethiopia is one of the countries which is frequently been exposed to extreme drought and famine throughout human history (2). The impact of drought in Ethiopia has been documented since 1974 (Web and Braun, 1990). However, numerous studies indicate that not all parts of Ethiopia have a history of recurrent drought events. According to Web and Braun (1990), the South-Eastern, Southern, North-Eastern (Afar), and Northern (Tigray Regional States) are the most affected by recurrent drought and famine. Henceforth, the Tigray and Afar regions are the regions repeatedly affected by recurrent drought events (Gebrekiros et al., 2016). Web and Braun (1990) also added that out of the 26 drought events that occurred between 1800 and 1990, Tigray region experienced up to 22 drought counts. Drought monitoring in Ethiopia shows moderate drought severity and a decline in drought magnitude from 2016 to 2019, however, it should be worth noting that, the mild wet period is insufficient to support ecosystem balance and crop yield production (Nasir et al., 2021). Other authors also documented a high drought magnitude, intensity and frequency of drought in the Tigray livelihood areas (Tefera et al, 2019; Rubangakene 2018). The IPCC (2015) report shows that many crop production areas in the next decade shall experience a more frequent and severe drought magnitude.

Tigray region is dry for most of the year except during the short rainy season and exhibits a semi-arid climate, making the agro-ecosystem highly sensitive to rainfall fluctuations; even a

This manuscript is a preprint and has not been peer reviewed. The copyright holder has made the manuscript available under a Creative Commons Attribution 4.0 International (CC BY) license and consented to have it forwarded to EarthArXiv for public posting.

slight change has a large impact on the socio-economic activities of the region (Tefera et al., 2019). The region's drought prone nature is attributed by high temperature and dry wind (Etsay et al, 2022). Both high temperature and dry wind have negative impact on crop yield (Asseng et al., 2016). Unforeseen crop yield loss and upsurge in food prices, chronic hunger is induced by drought (Cottrell et al., 2019; He et al., 2019; Asheber, 2010; Devereux & Sussex, 2000). The repercussion of drought is a translation of failure of early warning, community action, disaster preparation and dearth of external support (Orimoloye, 2022). Coupled with global warming, the impacts of drought events in the future climate of the Tigray region will possibly be worse than ever before. The steps to secure the future of the inhabitants of this region are to understand the future climate of the area and predict probable drought events. Understanding the drought events and their characteristics under the future climate of the study area is crucial for the timely preparation and development of early warning systems. Henceforth, this study examined the magnitude, duration and intensity of meteorological drought events from mid-term up to the end of the century (2099), using common and robust meteorological drought indices (SPI and SPEI) to generate information that can enhance proactive measures against future drought events.

2. Materials and Methods

2.1. Study area description

The study was conducted in the Kilte Awulaelo, Atsbi Wenberta and Gulomekeda districts, located in the Eastern zone of the Tigray region, Northern Ethiopia, with the coordinates: Latitude= 13° 33′ 1.96″ up to 14° 41′ 1.43″ N, Longitude= 39° 11′ 43.23″ up to 39° 59′ 41.24″ E. The altitude of the study area ranges from 1982 to 2666 meters above sea level (Table 1). The rainfall of this area is bimodal, with 80% of the total rainfall occurring from June to September

This manuscript is a preprint and has not been peer reviewed. The copyright holder has made the manuscript available under a Creative Commons Attribution 4.0 International (CC BY) license and consented to have it forwarded to EarthArXiv for public posting.

(JJAS) and the remaining 20% spread over the rest of the months. The annual rainfall ranges between 500mm and 800mm. Smallholder agriculture dominates the population's livelihood portfolio (Manaye et al., 2023).

Table 1: Study area locations (Universal Transverse Mercator coordinate system) and altitude

District	Synoptic Stations	Easting (m)	Northing (m)	Altitude (m.a.s.l)
Atsbi Wenberta	Atsbi	579048.81	1532324.33	2666
Gulomekeda	Fasti	541566.00	1592364.00	2567
Kilte Awulaelo	Wukro	564759.66	1522991.81	1982

2.2. Baseline meteorological data preparation and quality checks

The 30-year (1980 - 2009) observed meteorological datasets used in this study were obtained from the Ethiopian National Metrological Agency (NMA). However, the obtained meteorological datasets had some missing values thus, data gap-filling was required. The Statistical Downscaling Model (SDSM) in combination with the bias-correction method was employed. The observed meteorological datasets were bias-corrected using a comprehensive set of daily weather data acquired from the AgMIP (Agricultural Model Intercomparison Project). The gap-filled datasets were then checked for any discontinuity and bounds using TAMET software.

2.3. Future climate of the study area

This manuscript is a preprint and has not been peer reviewed. The copyright holder has made the manuscript available under a Creative Commons Attribution 4.0 International (CC BY) license and consented to have it forwarded to EarthArXiv for public posting.

The historical climate data and the future Global Climate Model data of Coupled Model Intercomparison Phase 5 (CMIP5) were used. The delta scenarios were created from CMIP5 GCMs and Bias Corrected Spatially Downscaled dataset using the "R" script "agmipsimple delta.R" following the guide for running AgMIP Climate Scenario Generation Tools with R in Windows (Hudson & Ruane, 2013). For each long-term (30-year) baseline dataset, the above script was used to create 80 delta-adjusted data files (2-time scales * 2 RCPs [4.5 and 8.5] * 20 GCM). The results were organized and presented using R software's boxplots and probability density functions (PDF). Therefore, the predicted future climate datasets were extracted in R software, and afterwards, climate model ensembles were created using the pivot table function of Excel. The use of climate ensembles was intended to overcome uncertainties in prediction that could result from differences in model parameterizations. The use of ensembles enables estimations of the certainty of results (Wilcke and Barring, 2016). The ensembled future climate datasets for mid-term (2040-2069) and end-term (2070-2099) for each of the stations were then used as inputs for SPI and SPEI computation.

We executed the correlation coefficient (r) test to evaluate the predictive performance of the GCMs, as applied in Adib et al. (2023), using equation one (1) below. The correlation coefficient was executed between the six (6) years of observed meteorological datasets [2011-2016] and the predicted meteorological datasets for the same period.

$$r = \frac{\sum(X_p - \overline{X}_p)(X_o - \overline{X}_o)}{\sqrt{\sum(X_p - \overline{X}_p)^2 \sum (X_o - \overline{X}_o)^2}} \quad (1)$$

This manuscript is a preprint and has not been peer reviewed. The copyright holder has made the manuscript available under a Creative Commons Attribution 4.0 International (CC BY) license and consented to have it forwarded to EarthArXiv for public posting.

Where: X_p and X_o represents predicted and observed values, respectively. $\overline{X}_p$ and $\overline{X}_o$ represents the average values of the predicted and observed, respectively.

2.4. Data analysis method

2.4.1. Meteorological drought events in the past and future climate of the study area

A meteorological drought is defined as a lack of precipitation over a region for a period. It is often defined based on the degree of dryness (in comparison to some "normal" or average amount) and the duration of the dry period (3). Within the scope of this study, station-based metrological drought was analyzed using the Standardized Precipitation Index (SPI) and the Standardized Precipitation and Evapotranspiration Index (SPEI) (4).

Standardized Precipitation Index (SPI) algorithm and interpretation

The SPI is an index based on the probability distribution of precipitation. It depends on the fitted density probability function, the length of the series used to estimate the parameters of the probability function and the method of estimation. Conceptually, SPI is equivalent to the *Z*-score used in statistics and is formulated in equation number two (2), as;

$$SPI\ ij = \frac{X\ ij - \mu\ ij}{\sigma\ ij} \qquad (2)$$

Where, SPI_{ij} is the SPI of the i^{th} month at j^{th} time-scale, X_{ij} is precipitation total for the i^{th} month at j^{th} time-scale, μ_{ij} and σ_{ij} are long-term mean and standard deviations associated with i^{th} month at j^{th} time-scale respectively. The SPI was designed to quantify the

This manuscript is a preprint and has not been peer reviewed. The copyright holder has made the manuscript available under a Creative Commons Attribution 4.0 International (CC BY) license and consented to have it forwarded to EarthArXiv for public posting.

precipitation deficit for multiple timescales. These timescales reflect the impact of drought on the availability of different water resources (3).

Since precipitations often do not follow a normal distribution (5), practical applications of the above SPI algorithm reveal some disadvantages (5, 6) such as misleadingly large positive or negative SPI values when the index is applied at short time steps to regions of low seasonal precipitation (7). To counteract this challenge, we considered computing the SPI by fitting the monthly long-term precipitation time series into a gamma parameter distribution to estimate the precipitation probability density functions (PDFs) as suggested by Thom (8). The gamma distribution is defined by its frequency or probability density function as expressed in equation three (3):

$$g(x) = \frac{1}{\beta^{\alpha}\,\Gamma(\alpha)} x^{\alpha-1} e^{x/\beta} \quad for\ x > 0 \qquad (3)$$

Where:

$\alpha > 0$ is a shape parameter, $\beta > 0$ is a scale parameter, $x > 0$ is the amount of precipitation and $\Gamma(\alpha)$ defines the gamma function, as expressed in equation four (4);

$$\Gamma(\alpha) = \int_0^{\infty} e^{-t} t^{\alpha-1}\, dt \qquad (4)$$

To fit the gamma distribution [g(x)] to the precipitation data (x), α and β are estimated for each time step of interest and each month of the year using the approximation of Thom (8) for maximum likelihood (9), as expressed in equations five (5) and six (6)

$$\hat{\alpha} = \frac{1}{4A}\left(1 + \sqrt{1} + \frac{4A}{3}\right) \qquad (5)$$

This manuscript is a preprint and has not been peer reviewed. The copyright holder has made the manuscript available under a Creative Commons Attribution 4.0 International (CC BY) license and consented to have it forwarded to EarthArXiv for public posting.

Where; $\hat{\alpha} = estimated\ alpha, A = \ln(x) - \frac{\ln \sum(x)}{n}$

$n = number\ of\ precipitation\ observations,$

$$\hat{\beta} = \frac{\bar{x}}{\hat{\alpha}} \qquad (6)$$

Where; $\hat{\beta} = estimated\ beta,\ \bar{x} =$ mean of precipitation data (x)

Integrating the probability density function $[g(x)]$ with respect to x and inserting the estimates of α and β yield an expression for the cumulative probability $G(x)$ of an observed amount of precipitation occurring for a given month and time step is shown using equation seven (7):

$$G(x) = \int_0^x g(x)dx = \frac{1}{\beta^{\alpha}\,\Gamma(\alpha)} x^{\alpha-1} e^{x/\beta} dx \qquad (7)$$

Since the gamma distribution is undefined for x=0 and q= P (x=0) > 0 where P (x=0) is the probability of zero precipitation, the cumulative probability will become as expressed using equation eight (8):

$$H(x) = q + (1 - q)G(x) \qquad (8)$$

The cumulative probability distribution was then transformed into the standard normal distribution to yield the SPI using the approximate conversion provided by (10)) expressed using equations nine (9) and ten (10) respectively;

for $0 < H(x) < 0.5$

This manuscript is a preprint and has not been peer reviewed. The copyright holder has made the manuscript available under a Creative Commons Attribution 4.0 International (CC BY) license and consented to have it forwarded to EarthArXiv for public posting.

$$z = SPI = -\left(t - \frac{c_0 + c_1 t + c_2 t^2}{1 + d_1 t + d_2 t^2 + d_3 t^3}\right), t = \sqrt{ln\left(\frac{1}{(H)(x)^2}\right)} \quad (9)$$

for $0.5 < \mathrm{H}(x) < 1.0$

$$z = SPI = +\left(t - \frac{c_0 + c_1 t + c_2 t^2}{1 + d_1 t + d_2 t^2 + d_3 t^3}\right), t = \sqrt{ln\left(\frac{1}{(1.0 - H)(x)^2}\right)} \quad (10)$$

$Where; c_0$ = 2.515517; c_1 = 0.802853; c_2 = 0.010328; d_1=1.432788; d_2 = 0.189269; d_3 = 0.001308

Standardized Precipitation and Evapotranspiration Index (SPEI)

Although precipitation is the primary factor controlling the formation and persistence of drought, other variables, such as evapotranspiration (negative impact), impose greater penalties on the SPI model (Rojas et al., 2019; Lee et al., 2017). SPEI is one of the climatic proxies widely used for drought quantification and monitoring (11). The inputs required to run the program are precipitation, mean temperature, terrestrial radiation and latitude of the study site(s). The index was developed by Vicente-Serrano et al. (2010) to address the issue of potential evapotranspiration (PET) by including a temperature component in the quantification and monitoring of drought scenarios. The SPEI uses the monthly (or weekly) difference between precipitation (P) and *PET*. This represents a simple climatic water balance, which is calculated at different time scales to obtain the SPEI. In this research, the *PET* was computed using Hargreaves' method (Hargreave, 1989) shown in equation eleven (11):

$$\mathrm{ET}_0 = 0.0023 * Ra * \mathrm{Sqrt}(\mathrm{TD}) * (\mathrm{TA} + 17.8) \quad (11)$$

This manuscript is a preprint and has not been peer reviewed. The copyright holder has made the manuscript available under a Creative Commons Attribution 4.0 International (CC BY) license and consented to have it forwarded to EarthArXiv for public posting.

Where;

$TD = Temperature\ difference$

$TA = Average\ temperature$

$Ra = Extra\ terrestrial\ radiation$

With a value for *PET*, the difference (*D*) between the precipitation (*P*) and potential evapotranspiration (*PET)* for the $month_i$, will be calculated using equation twelve (12) as:

$$D_i = P_i - PET_i \quad (12)$$

Standardization of the variable for SPEI computation

Log-logistic distribution was used to standardize the variables. The probability density function of a three-parameter Log-logistic distributed variable is expressed using equation thirteen (13) as:

$$f(x) = \frac{\beta}{\alpha}\left(\frac{x-\gamma}{\alpha}\right)^{\beta-1}\left(1+\left(\frac{x-\gamma}{\alpha}\right)^{\beta}\right)^{-2} \quad (13)$$

, where α, β and γ are scale, shape, and origin parameters, respectively, for *D* values in the range ($\gamma > D < \infty$).

Positive SPI/SPEI values indicate greater than median precipitation, and negative values indicate less than median precipitation (11). Because the SPI/SPEI is normalized, wetter and drier

This manuscript is a preprint and has not been peer reviewed. The copyright holder has made the manuscript available under a Creative Commons Attribution 4.0 International (CC BY) license and consented to have it forwarded to EarthArXiv for public posting.

climates can be represented in the same way (11); thus, wet periods can also be monitored using the SPI/SPEI. Once standardized, the strength of the SPI and SPEI, is given in table 2.

Table 2: SPI/SPEI values

SPI/SPEI	Severity level
2.0+	Extremely wet
1.5 to 1.99	Very wet
1.0 to 1.49	Moderately wet
-.99 to .99	Near Normal
-1.0 to -1.49	Moderately dry
-1.5 to -1.99	Severely dry
-2 and less	Extremely dry

Source: Vicente-Serrano et al., (2010)

In this study, a 4 and 12-month time scale SPI and SPEI were calculated using the historical and predicted meteorological datasets of the future climate for the study area. A 4-month SPI and SPEI reflect short- and medium-term moisture conditions (4). In other words, a 4-month SPI and SPEI at the end of September compares the June–July–August–September precipitation total in that particular year with the June–September precipitation totals of all the 30 years on record for the study area (4). Since the Eastern Tigray zone is a primary agricultural area for the region (13), a 4-month SPI and SPEI shall be more effective in highlighting moisture conditions during cropping cycles. On the other hand, the 12-month SPI and SPEI compare precipitation for 12 consecutive months with that recorded in the same 12 consecutive months in all 30 years

This manuscript is a preprint and has not been peer reviewed. The copyright holder has made the manuscript available under a Creative Commons Attribution 4.0 International (CC BY) license and consented to have it forwarded to EarthArXiv for public posting.

recorded for the study area. The 12-month SPI/SPEI highlights the hydrological impacts of drought (4).

2.4.2. Quantifying metrological drought magnitude, duration and intensity in the past and future climate

Using the output from SPI and SPEI, the drought magnitude, duration, and mean intensity in the future climate of the study area were analyzed using the following equations:

Drought Magnitude

This was analyzed using the following equation fourteen (14)

$$DM = -\left(\sum_{x=j}^{x} SPI_i\right) \quad (14)$$

Where:

- DM – Drought Magnitude;

- j – the first month of the dry event;

- x – last month of the dry event;

- SPI_i– SPI values of jx sequences calculated over a period of x months.

A drought event occurs any time the SPI is continuously negative with an intensity of less than or equal to -1.0. The event ends when the SPI becomes positive. In this method of drought analysis, the drought magnitudes are the positive sums of the SPI values that are continually negative over consecutive months (14).

This manuscript is a preprint and has not been peer reviewed. The copyright holder has made the manuscript available under a Creative Commons Attribution 4.0 International (CC BY) license and consented to have it forwarded to EarthArXiv for public posting.

Drought Duration

The duration of a drought event is calculated as the difference between the moment of its beginning and that of its ending using equation fifteen (15).

$$DD = t_2 - t_1 \quad (15)$$

Where DD is the drought duration, t_2 is the drought episode cessation time (month), and t_1 is the drought episode onset time (month)

Drought Intensity

This was analysed using equation sixteen (16)

$$DI = \frac{DM}{DD} \quad (16)$$

Where; DM is the drought magnitude, DD refers to the drought duration.

2.4.3. SPI and SPEI processing methodology

R software version 3.4.0 (15) was used for the computation of SPI. R-scripts developed with rectangular kernel type, gamma distribution and "ub-pwm" fit in Tinn-R software were used for calculating SPI. The Standardized Precipitation-Evapotranspiration Index was computed using the R-scripts provided by Vicente-Serrano, Begueria (11). The script was developed with Log-logistic distribution for standardization and rectangular kernel function for smoothing noisy SPEI.

3. Results

3.1. Climate of the study area

This manuscript is a preprint and has not been peer reviewed. The copyright holder has made the manuscript available under a Creative Commons Attribution 4.0 International (CC BY) license and consented to have it forwarded to EarthArXiv for public posting.

The study observed a moderately strong and positive (0.62, 0.6 and 0.67) correlation coefficient (r) value for evaluating the predictive performance of the GCMs executed between the six (6) years of observed meteorological datasets [2011-2016] and the predicted meteorological datasets for the same period for Atsbi, Fatsi and Wukro stations, respectively.

The mean annual rainfall over the past 30 years (1980 - 2009) in Fatsi, Atsbi and Wukro stations was 645 mm, 800 mm, and 601 mm, respectively. The greatest proportion of rainfall was received in the kiremt season (JJAS) (Fig1), and the total amount received during the main growing season was relatively lower in Fatsi compared to Wukro and Atsbi. Additionally, spatial-temporal variability in peak rainfall during the main rainy season was observed over the study area, with Wukro and Fatsi receiving peak rainfall in July as opposed to August for Atsbi station. The probability of getting Kiremt season rainfall of greater than 300 mm was 40% of the year in Atsbi and Wukro and 30% of the year in Fatsi. The daily mean air temperature (Tmean) recorded for Wukro, Atsbi and Fatsi stations are 18.55 °C, 14.6 °C and 18.4 °C, respectively. Evaporative demand of the atmosphere (mm day-1), which is directly influenced by the average air temperature of the study area, is presented using probability density curves (Fig 2).

This manuscript is a preprint and has not been peer reviewed. The copyright holder has made the manuscript available under a Creative Commons Attribution 4.0 International (CC BY) license and consented to have it forwarded to EarthArXiv for public posting.

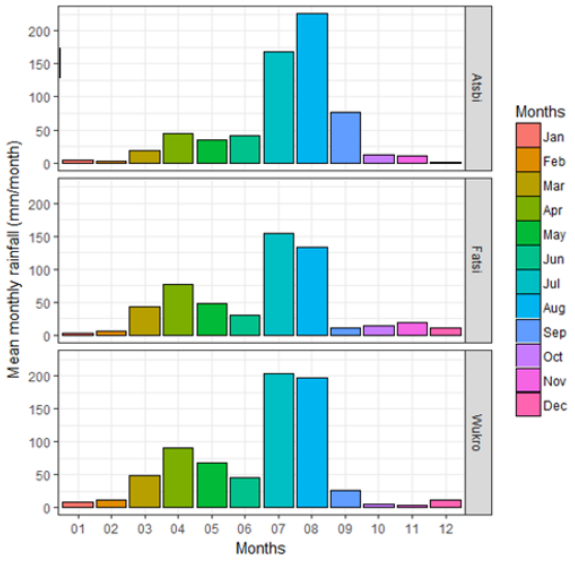

Fig 1: Monthly precipitation pattern of the study area

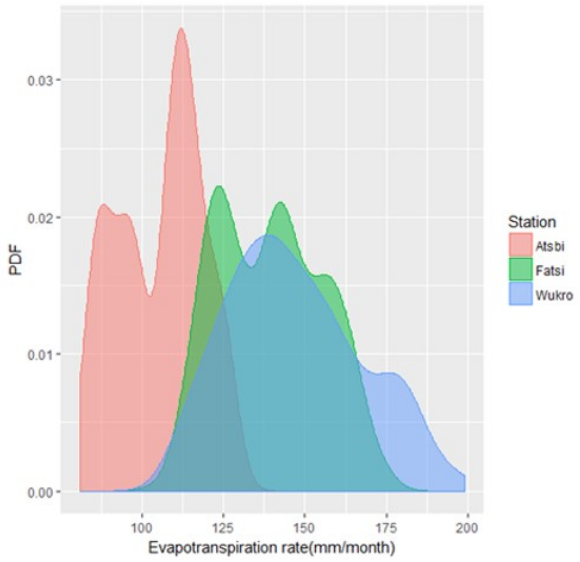

Fig 2: Probability density functions of potential evapotranspiration derived from 30-year historical climate data of the study area

2.5. Temperature and rainfall outlook in the future climate of the study area

2.5.1. Daily mean air temperature [T_{mean}]

The projected change in daily mean air temperature [Tmean] is presented in Fig 3. Considering Atsbi station, the T_{mean} is predicted to increase above the baseline by +1.605 ˚C during MT RCP 4.5, and by +2.77 ˚C under MT RCP 8.5. Under ET RCP 4.5, an exceedance above the baseline is +2.305 ˚C. Under the ET RCP 8.5, the T_{mean} increased by up to +4.77 ˚C above the baseline (Fig 3). At Wukro station, the T_{mean} is shown to increase by +1.985 ˚C above the baseline during MT RCP 4.5, and +2.58 ˚C under MT RCP 8.5. Under ET RCP 4.5, T_{mean} increased by +2.22 ˚C and, in the ET RCP 8.5, an exceedance of up to +3.95 ˚C was projected. At Fatsi station, the T_{mean} is projected to increase above the baseline by +1.85 ˚C during MT RCP 4.5, and

This manuscript is a preprint and has not been peer reviewed. The copyright holder has made the manuscript available under a Creative Commons Attribution 4.0 International (CC BY) license and consented to have it forwarded to EarthArXiv for public posting.

+2.55 ˚C, at MT RCP 8.5. Under ET RCP 4.5, an exceedance above the baseline was found to be +2.18 ˚C, and at ET RCP 8.5, an increase above the baseline by +4.05 ˚C was projected.

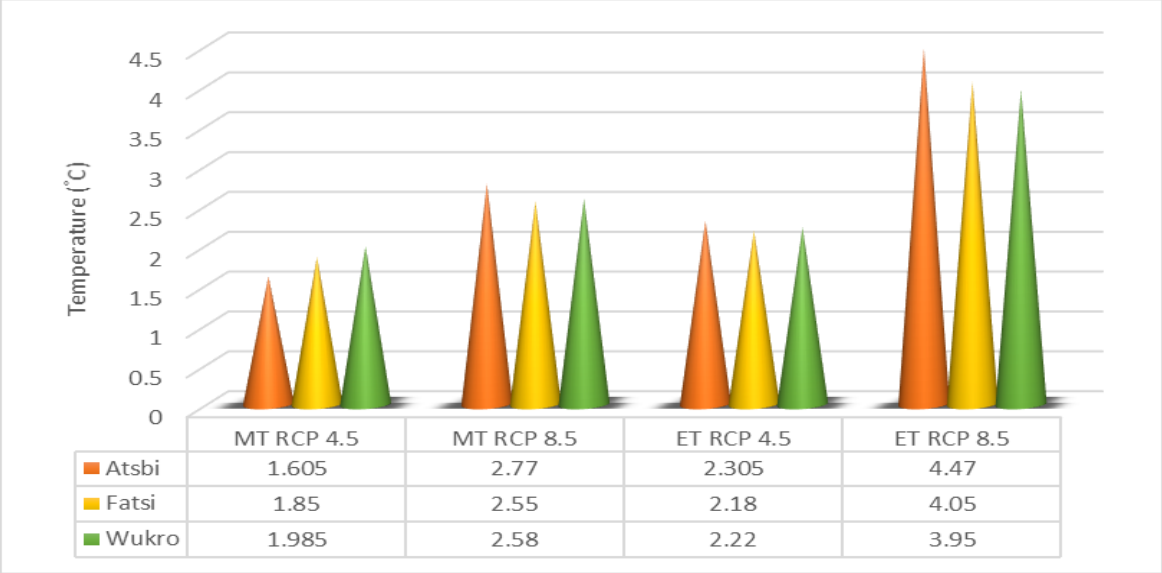

	MT RCP 4.5	MT RCP 8.5	ET RCP 4.5	ET RCP 8.5
Atsbi	1.605	2.77	2.305	4.47
Fatsi	1.85	2.55	2.18	4.05
Wukro	1.985	2.58	2.22	3.95

Fig 3: Daily mean temperature (°C) exceedance (+) above baseline value for the study area

2.5.2. Predicted change in mean rainfall (mm annum^{-1})

In Atsbi Station, annual precipitation is expected to change relative to the baseline value by +19.09% under MT RCP 4.5, +18.34% under MT RCP 8.5, +14.22% at ET RCP 4.5 and +50.69% at ET RCP 8.5. At Wukro Station, the mean annual rainfall is predicted to change relative to the baseline value by +4.97% under MT RCP 4.5, +11.32% under MT RCP 8.5, +10.76% in ET RCP 4.5 and +47.62% at ET RCP 8.5, respectively. In Fatsi Station, the mean annual rainfall is changed relative to the baseline value by +4.54% under MT RCP 4.5, +9.78% under MT RCP 8.5, +10.02% at ET RCP 4.5 and +45.55% at ET RCP 8.5.

2.5.3. Meteorological drought events and their characteristics in the past and future climate of the study area

This manuscript is a preprint and has not been peer reviewed. The copyright holder has made the manuscript available under a Creative Commons Attribution 4.0 International (CC BY) license and consented to have it forwarded to EarthArXiv for public posting.

Drought magnitude, duration and intensity under the past and future climate of the study area were computed based on SPI and SPEI indices outputs. Fig 4 shows the meteorological drought stress (Red spikes) under the future climate of the study area based on SPI and SPEI indices. The depth of the red spikes on the graphics directly measures the intensity of the climate condition—drought — being assessed for that period. The drought intensity (depth of the red spikes) is a function of precipitation deficit, evapotranspiration (The case of SPEI) and duration of the drought event.

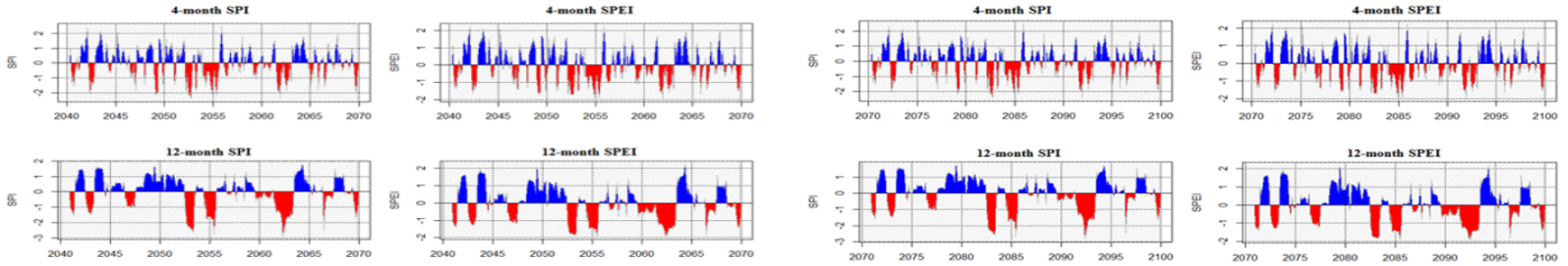

Atsbi Station

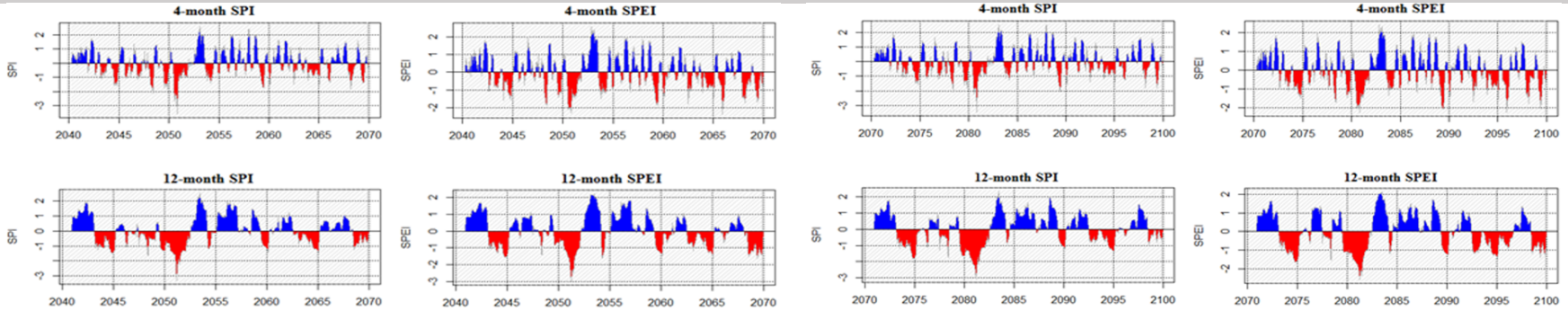

Fatsi Station

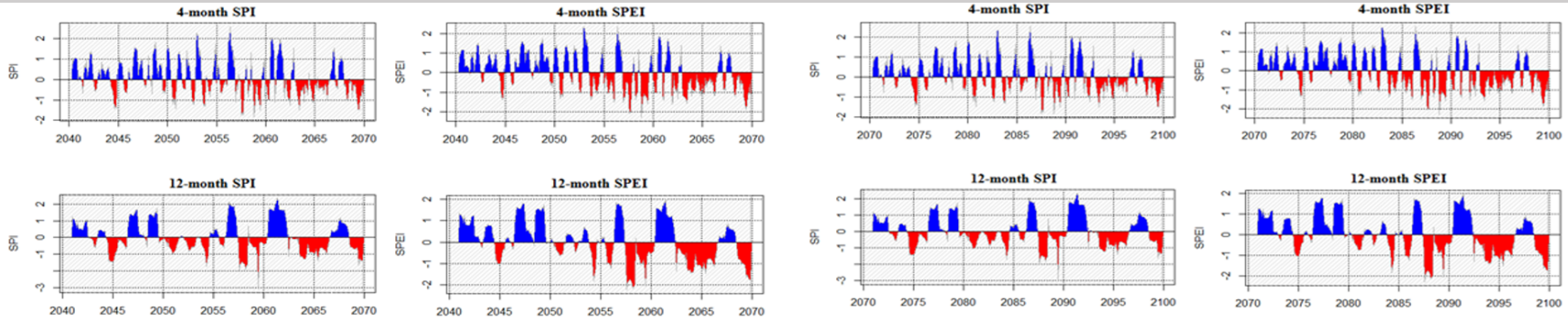

Wukro Station

Fig 4: Meteorological drought stress (Red spikes) under the future climate of the study area based on SPI and SPEI indices

1

This manuscript is a preprint and has not been peer reviewed. The copyright holder has made the manuscript available under a Creative Commons Attribution 4.0 International (CC BY) license and consented to have it forwarded to EarthArXiv for public posting.

2.6. Drought Magnitude (DM)

2.6.1. Drought Magnitude under past climate (1980-2009)

The magnitude of a considered drought event corresponds to the cumulative precipitation deficit over the drought period. Based on the SPI-4 and SPEI-4 indices, the highest magnitude of short-term drought in Fatsi was -11.8. The drought event that yielded this highest magnitude occurred in 1990 and lasted eight consecutive months. Atsbi, on the other hand, experienced the highest magnitude (-18.7) of short-term drought in 1997. The drought event contributing to this magnitude lasted for 10 consecutive months. Considering Wukro, the highest drought magnitude (-8.83) occurred during the drought event of the year 2003. The drought that caused this magnitude lasted for 5 consecutive months. Focusing on SPI-12 and SPEI-12 indices (long-term drought), Fatsi, experienced the highest magnitude (-53) during the drought events of 1989-1992, which lasted for 31 consecutive months. In the following year (1993), Atsbi experienced the highest magnitude of long-term drought (-21.7) in a drought event that lasted for 15 consecutive months. Wukro, on the other hand. experienced the highest magnitude of long-term drought during the drought event of 1997 which lasted for 20 consecutive months with a corresponding magnitude of -25.9. Looking at the total drought magnitude for each of the three stations, Atsbi and Wukro experienced a higher magnitude (DM > -75) compared to Fatsi, focusing on short-term drought (SPI/SPEI-4 timescale). Atsbi and Fatsi experienced the highest total magnitude (DM > -87) of long-term drought compared to Wukro. Consequently, Atsbi experienced a high magnitude of both short-term and long-term drought during the baseline years.

2.6.2. Total Drought Magnitude under future climate (2040-2099)

The total drought magnitude under the future climate (2040-2099) of the study area is shown in Fig 5. Based on Fig 5-A, both SPI-4 and SPEI-4 showed that a higher magnitude of short-term drought will be experienced in Atsbi and Wukro compared to Fatsi. Considering long-term drought (Fig 5-B), SPI-12 and SPEI-12 showed relatively higher total magnitude in Atsbi and Fatsi than in Wukro. Comparatively, Atsbi

This manuscript is a preprint and has not been peer reviewed. The copyright holder has made the manuscript available under a Creative Commons Attribution 4.0 International (CC BY) license and consented to have it forwarded to EarthArXiv for public posting.

will likely experience a higher total magnitude of both short-term and long-term drought under the future climate.

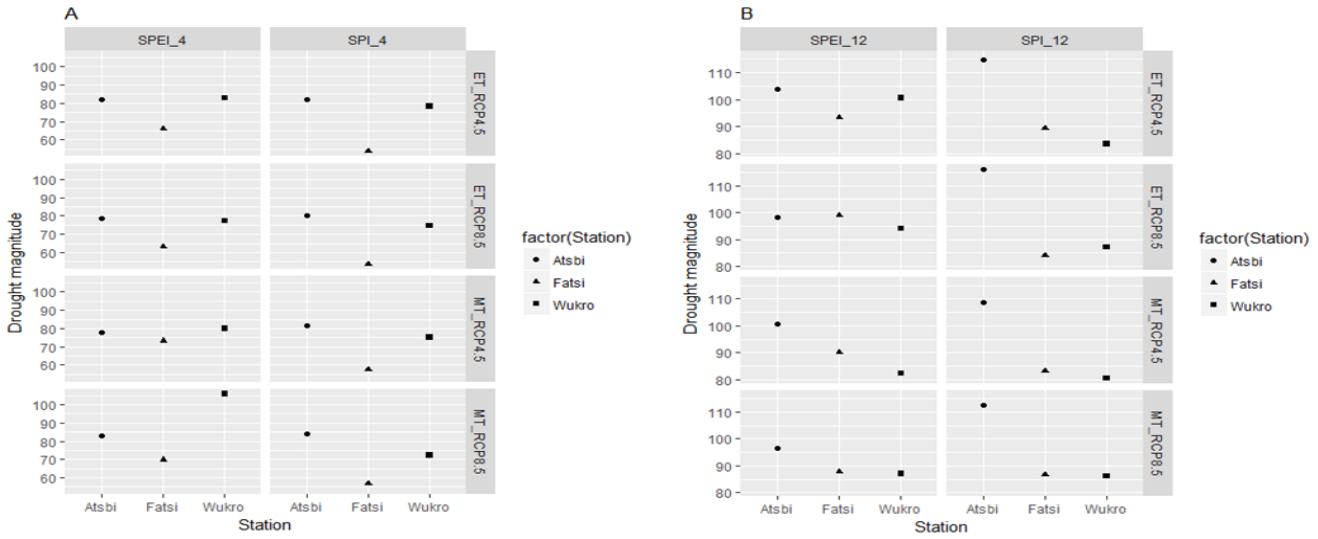

Fig 5: Predicted drought magnitude under future climate

2.6.3. Total Drought Magnitude trend in the future relative to the baseline.

To ascertain whether there will be a decline or escalation in drought magnitude under future climate relative to the baseline value, computation of the difference between drought magnitude under past and future climate of the study area was done to discover the pattern of change. Fig 6 illustrates the general pattern of change in drought magnitude under the future climate relative to the baseline value. All the positive values depict an upsurge, negative values show a decline in drought magnitude, and zero shows neither increase nor decrease relative to the baseline.

This manuscript is a preprint and has not been peer reviewed. The copyright holder has made the manuscript available under a Creative Commons Attribution 4.0 International (CC BY) license and consented to have it forwarded to EarthArXiv for public posting.

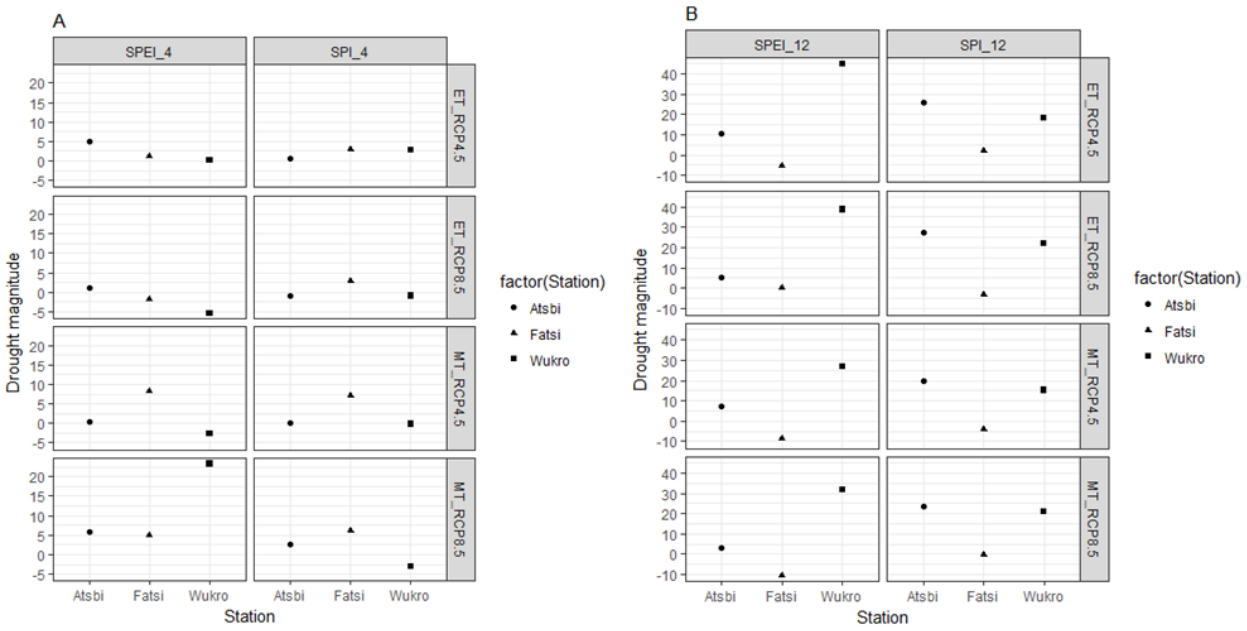

Fig 6: Predicted drought magnitude trend relative to the baseline

Based on SPI-4, the result demonstrates that Fatsi will likely experience a greater increase in the magnitude of short-term drought than Atsbi and Wukro in all time segments (Mid-terms and End-terms) and emission scenarios (RCPs). A greater upsurge in Fatsi's drought magnitude (-7.0 and -6.1) will occur during MT under both RCPs. In Atsbi, the deviation of future drought magnitude from the baseline values was found to be minimal except at midterm, RCP 8.5 and end-term, RCP 4.5, as indicated by SPI-4 timescale. Wukro, on the other hand, is expected to experience an increase in the magnitude of short-term drought (+23 and +2.9) only during midterm, RCP 8.5 and end-term RCP 4.5 as registered by SPEI-4 and SPI-4, respectively.

Considering long-term drought, Atsbi and Wukro will likely experience a greater upsurge in total drought magnitude than Fatsi. Both the SPEI-12 and SPI-12 revealed a rise in drought magnitude under all-time segments (Mid-terms and End-terms) and emission scenarios (RCPs), although the increase exhibited by SPEI-12 is superior to SPI-12. Though relatively lower than that of Wukro, Atsbi will experience an upsurge under all-time segments and emission scenarios except during midterm, RCP 4.5 and end-term RCP 4.5 based on SPI-12. Fatsi will generally experience a decline in the magnitude of long-term drought except under ET RCP 4.5.

This manuscript is a preprint and has not been peer reviewed. The copyright holder has made the manuscript available under a Creative Commons Attribution 4.0 International (CC BY) license and consented to have it forwarded to EarthArXiv for public posting.

3.4. Drought Duration (DD)

3.4.1. Total Drought Duration under past climate (1980-2009)

Drought duration is closely linked to its onset and cessation date and is sometimes expressed in terms of the number of consecutive months of precipitation deficit. Comparatively, a higher duration of short-term drought was experienced in Wukro and Atsbi during the past 30 years than Fatsi based on both SPEI-4 and SPI-4 timescales. It was also observed that for all three stations, at least 30 out of 360 months experienced short-term drought phenomena and up to 40 out of 360 months suffered long-term drought. The longest duration of short-term drought in Wukro, Atsbi and Fatsi occurred during the drought events of 1997, 1993/1997 and 1991, respectively. On the contrary, the longest long-term drought duration (months) was observed in Atsbi and Fatsi than in Wukro based on the SPEI-12 and SPI-12 timescales. SPEI-12 timescale explained slightly higher drought duration (months) in all three stations compared to SPI-12.

3.4.2. Total Drought Duration trend in the future relative to the past

The number of consecutive months with precipitation deficit under the future climate is shown in Fig7.

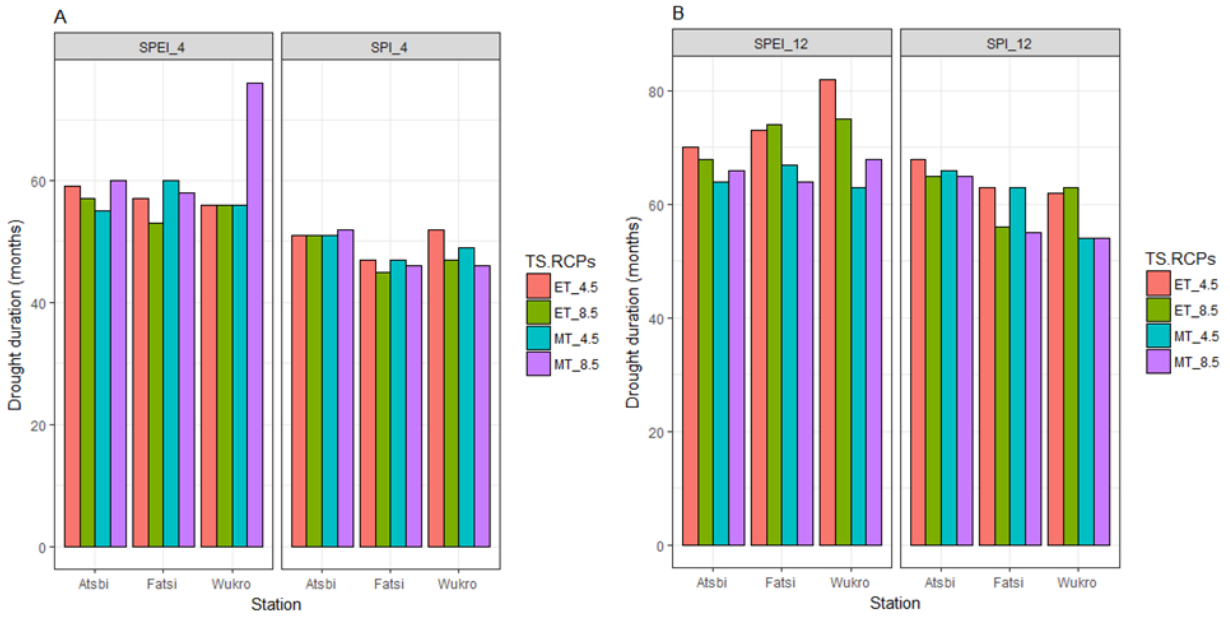

Fig 7: Predicted Total Drought Duration under future climate

This manuscript is a preprint and has not been peer reviewed. The copyright holder has made the manuscript available under a Creative Commons Attribution 4.0 International (CC BY) license and consented to have it forwarded to EarthArXiv for public posting.

For better comprehension of the trend relative to the baseline, computation and graphical illustration of the trend of change relative to the baseline were performed (Fig 8). The legend title (TS. RCPs) denotes time segments and emission scenarios. Considering short-term drought, the total number of consecutive dry months is expected to increase more in Fatsi based on both the SPEI-4 and SPI-4 timescales. Wukro, on the other hand, will experience a reduction in the number of months with short-term drought under future climate, except in MT RCP 8.5 and end-term 4.5, as shown by SPEI-4 and SPI-4, respectively. Looking at long-term drought, Wukro will experience the greatest increase in consecutive dry months in all-time segments and emission scenarios. However, a greater increase in the duration of long-term drought will be experienced at the end of the century, as shown using both SPEI-12 and SPI-12. Atsbi will also experience a slight increase in the number of months with long-term drought, though much lower than that of Wukro. Fatsi, on the other hand, will experience a decline in the number of months experiencing long-term drought during the midterm, especially as shown by SPEI-12 indices output.

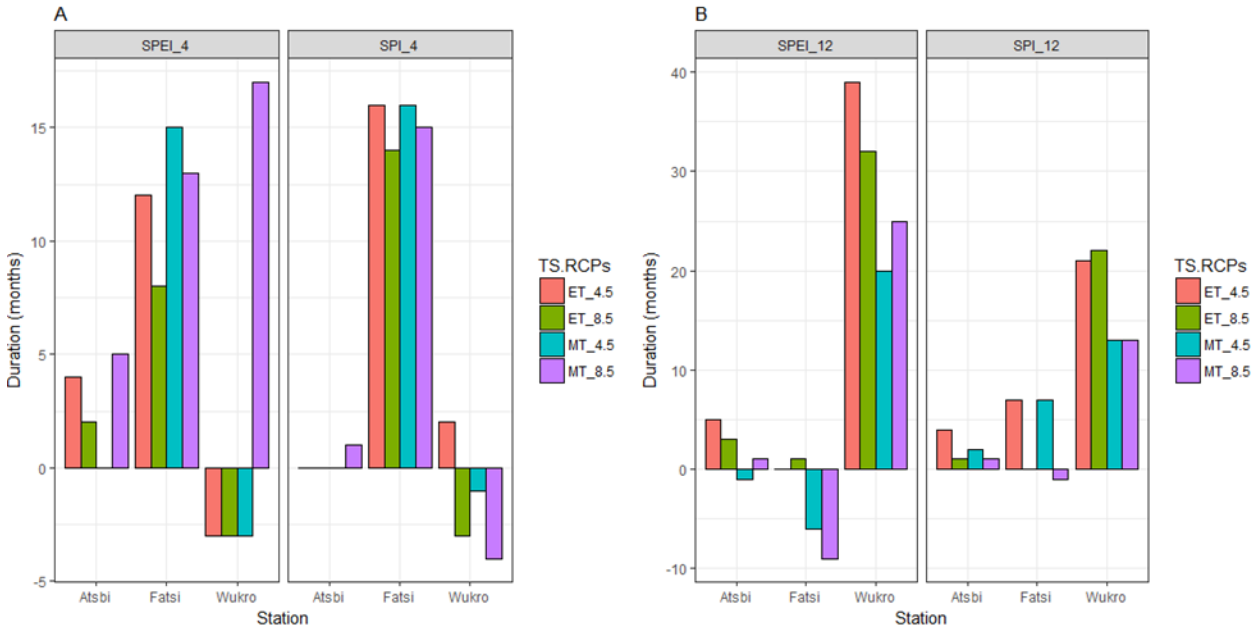

Fig 8: Predicted drought duration trend under future climate

3.4.3 Longest Drought Duration and Peak Intensity (including year) under the past climate

This manuscript is a preprint and has not been peer reviewed. The copyright holder has made the manuscript available under a Creative Commons Attribution 4.0 International (CC BY) license and consented to have it forwarded to EarthArXiv for public posting.

The longest drought episodes and peak intensity are shown in Table 3. In the past, Atsbi experienced a peak intensity of short- and long-term drought during the drought event of 1995. In Fatsi, the peak intensity of short- and long-term drought occurred during the drought events of 1990 and 1991, respectively. Wukro, on the other hand, experienced the highest drought intensity of short- and long-term drought in the years 1997 and 2009.

Table 3: Sampled meteorological drought characteristics under the past climate

Station	Longest Drought Duration (No. months/Year)		Peak intensity and the year	
	a	b	a	b
Atsbi	6 (1982)	21 (2001-2003)	-1.95 (1995)	-1.91 (1995)
Fatsi	8 (1988-1989)	19 (1990-1991)	-2.35 (1990)	-2.56 (1991)
Wukro	6 (1994)	20 (2007-2009)	-2.28 (2009)	-1.83 (1997)

a=Short-term drought, b=Long-term drought

3.4.4 Longest Drought Duration and Peak Intensity (including year) under future climate

In the future, Atsbi will likely experience peak intensity of short- and long-term drought during drought events of 2080 and 2082-2083, respectively (Table 4). In Fatsi, the peak intensity of short- and long-term drought will occur during the drought event of 2080-2081 and 2050-2052, respectively. Wukro, on the other hand, will experience the highest intensity of short- and long-term drought in the years 2069 and 2057-2059, respectively.

Table 4: Sampled meteorological drought characteristics under the future climate

Station	Longest Drought Duration (No. months/Year)		Peak intensity and the year	
	a	b	a	b
Atsbi	7 (2076-2077)	21 (2061-2063/2091-2093)	-2.06 (2080)	-1.69 (2082-2083)

This manuscript is a preprint and has not been peer reviewed. The copyright holder has made the manuscript available under a Creative Commons Attribution 4.0 International (CC BY) license and consented to have it forwarded to EarthArXiv for public posting.

Fatsi	7 (2080-2081)	31 (2079-2082)	-2.11 (2080-2081)	-1.65 (2050-2052)
Wukro	6 (2058-2059/ 2088-2089)	24 (2094-2096)	-2.22 (2069)	-1.57 (2057-2059)

a=Short-term drought, b=Long-term drought

3.5. Predicted timings of imminent drought events, including their magnitude and intensity.

The predicted timings of imminent drought events, including their magnitude and intensity for each location (station), are presented in Table 5-10. As indicated in Table 5, Atsbi will experience at least 29 counts of short-term drought with occurrences in the mid-term (2040-2069). A total of 102 months will experience drought events, with half of them occurring in the mid-term. The longest short-term drought duration will occur in the drought event of 2076-2077. This drought will likely last for 7 consecutive months. Considering long-term drought, Atsbi will experience at least 16 drought counts (9 in the mid-term and 7 in the end-term). A total of 138 months will experience long-term drought events, with 70 occurring in the mid-term. The longest drought event will last for 21 consecutive months, and this will probably occur in the years 2061-2063 as well as 2091-2093 (Table 6).

Fatsi will experience at least 19 short-term drought counts, with 10 events occurring in the mid-term and at least 9 in the end-term. A total of 71 months will experience short-term drought events, with 36 occurring in MT. The longest duration of short-term drought will be in the years 2050-2051 and 2080-2081, both lasting for at least 7 consecutive months (Table 7). Considering long-term drought, Fatsi will experience at least 19 drought counts (10 in the mid-term and 9 in the end-term). A total of 137 months will experience long-term drought events, with 64 occurring in the mid-term. The longest drought duration based on a 12-month SPI/SPEI scale will be in the years 2079-2082, lasting for at least 31 consecutive months (Table 8).

Wukro will experience at least 30 short-term drought counts (15 in the mid-term and 15 in the end-term). At least a total of 112 months will experience drought events, with 56 occurring in the mid-term. The longest short-term drought duration will be in the years 2058-2059 and 2088-2089, with each drought event lasting

This manuscript is a preprint and has not been peer reviewed. The copyright holder has made the manuscript available under a Creative Commons Attribution 4.0 International (CC BY) license and consented to have it forwarded to EarthArXiv for public posting.

for 6 consecutive months (Table 9). Considering long-term drought, Wukro will experience at least 14 drought events (7 in the mid-term and 7 in the end-term). A total of 143 months will experience long-term drought events, with 68 drought counts occurring in the mid-term. The longest drought duration based on a 12-month SPI/SPEI scale will occur in the drought event of 2094-2096, and it will last for 21 consecutive months (Table 10).

Table 5: Predicted Short-Term Drought Events under the Future Climate of Atsbi

Drought year	DD (months)	Inception	Termination	Tot. Magnitude	Mean Intensity
2040	2	Sep	Oct	-2.787855	-1.393928
2042	5	Jun	Oct	-7.254839	-1.450968
2046-2047	3	Dec	Feb	-4.216657	-1.405552
2049	4	Feb	May	-7.521924	-1.880481
2049	2	Nov	Dec	-2.769988	-1.384994
2052	2	Mar	Apr	-3.68278	-1.841390
2052	5	Jun	Oct	-10.05270	-2.010540
2053	3	Mar	May	-4.927645	-1.642548
2054	2	Apr	May	-2.680007	-1.340003
2054-2055	5	Sep	Jan	-7.213774	-1.442755
2055	3	Apr	Jun	-5.306782	-1.768927
2061	4	Sep	Dec	-7.636737	-1.909184
2062	5	Jun	Oct	-6.656889	-1.331378
2066	2	Jul	Aug	-2.632357	-1.316178
2069	4	Aug	Nov	-6.065469	-1.516367
2070	2	Sep	Oct	-2.872417	-1.436208
2072	6	May	Oct	-9.066845	-1.511141

This manuscript is a preprint and has not been peer reviewed. The copyright holder has made the manuscript available under a Creative Commons Attribution 4.0 International (CC BY) license and consented to have it forwarded to EarthArXiv for public posting.

2076-2077	7	Dec	May	-10.60518	-1.490291
2079	2	Nov	Dec	-2.637022	-1.318511
2082	2	Mar	Apr	-3.314251	-1.657126
2082	5	Jun	Oct	-10.34871	-2.069741
2083	3	Mar	May	-4.310656	-1.436885
2084	2	Apr	May	-2.666045	-1.333023
2084-2085	5	Sep	Jan	-6.886107	-1.377221
2085	3	Apr	Jun	-6.105155	-2.035052
2091	4	Sep	Dec	-7.382008	-1.845502
2092	4	Jul	Oct	-5.242595	-1.310649
2096	2	Jul	Aug	-2.619971	-1.309985
2099	4	Aug	Nov	-6.165279	-1.541320

Table 6: Predicted Long-Term Drought Under the Future Climate of Atsbi

Drought year	DD (months)	Inception	Termination	Tot. Magnitude	Mean Intensity
2040-2041	6	Dec	May	-7.394389	-1.232398
2043	5	Nov	Mar	-6.215700	-1.243140
2046-2047	5	Oct	Feb	-5.349038	-1.069808
2047	2	May	Jun	-2.313777	-1.156888
2052-2053	12	Jul	Jun	-19.90748	-1.658957
2054-2055	12	Sep	Aug	-18.71362	-0.155947
2061-2063	21	Sep	May	-30.42255	-1.448693
2066	2	Jul	Aug	-3.161030	-1.580515
2069	5	Aug	Dec	-6.346654	-1.269331
2070-2071	7	Dec	Jun	-8.715672	-1.245096

This manuscript is a preprint and has not been peer reviewed. The copyright holder has made the manuscript available under a Creative Commons Attribution 4.0 International (CC BY) license and consented to have it forwarded to EarthArXiv for public posting.

2072-2073	9	Aug	Apr	-12.10651	-1.345168
2082-2083	13	Jul	Jul	-21.99725	-1.692096
2084-2085	12	Sep	Aug	-18.45713	-1.538094
2091-2093	21	Sep	May	-28.93587	-1.377898
2096	2	Jul	Aug	-3.041779	-1.520889
2099	4	Sep	Dec	-5.048456	-1.262114

Table 7: Predicted Short-Term Drought Events Under the Future Climate of Fatsi 1

Drought year	DD (months)	Inception	Termination	Tot. Magnitude	Mean Intensity
2044	5	Jul	Nov	-7.408615	-1.481723
2048	4	Mar	Jun	-7.012735	-1.753184
2049	4	Aug	Nov	-6.480922	-1.620231
2050-2051	7	Jul	Jan	-14.80432	-2.114903
2054	3	Feb	Apr	-3.547012	-1.182337
2059	4	Apr	Jul	-6.156418	-1.539104
2060	2	Feb	Mar	-2.910334	-1.455167
2066	2	Jan	Feb	-2.517275	-1.258638
2068	2	Mar	Apr	-3.164299	-1.582150
2069	3	May	Jul	-3.724758	-1.241586
2074	5	Jul	Nov	-7.062609	-1.412522
2078	4	Mar	Jun	-6.093891	-1.523473
2079	5	Jul	Nov	-7.124922	-1.424984
2080-2081	7	Jul	Jan	-13.47867	-1.925524
2089	4	Apr	Jul	-6.600864	-1.650216
2090	2	Feb	Mar	-2.901082	-1.450541

This manuscript is a preprint and has not been peer reviewed. The copyright holder has made the manuscript available under a Creative Commons Attribution 4.0 International (CC BY) license and consented to have it forwarded to EarthArXiv for public posting.

2095-2096	3	Dec	Feb	-3.37796	-1.125987
2098	2	Mar	Apr	-2.998051	-1.499026
2099	3	May	Jul	-4.052713	-1.350904

Table 8: Predicted Long-Term Drought Events Under the Future Climate of Fatsi

Drought year	DD (months)	Inception	Termination	Tot. Magnitude	Mean Intensity
2043-2044	3	Dec	Feb	-3.508545	-1.169515
2044-2045	7	Aug	Feb	-9.969395	-1.424199
2048	2	May	Jun	-2.76499	-1.382495
2050-2052	18	Aug	Jan	-29.77711	-1.654284
2054	3	Apr	Jun	-4.521060	-1.507020
2059-2060	8	Aug	Mar	-9.851099	-1.231387
2064-2065	8	Jul	Feb	-10.12603	-1.125115
2068-2069	8	Jul	Feb	-9.954086	-1.244261
2069	3	May	Jul	-4.228591	-1.409530
2069	4	Sep	Dec	-5.364825	-1.341206
2073-2074	4	Dec	Mar	-4.353725	-1.088431
2074-2075	11	May	Mar	-16.39392	-1.490357
2078	2	May	Jun	-2.343936	-1.171968
2079-2082	31	Aug	Feb	-46.75865	-1.508343
2090	3	Jan	Mar	-3.088177	-1.029392
2092-2093	9	Aug	Apr	-10.95938	-1.217709
2094-2095	7	Aug	Feb	-8.165705	-1.166529
2099	3	May	Jul	-3.603574	-1.201191
2099	3	Oct	Dec	-3.188050	-1.062683

This manuscript is a preprint and has not been peer reviewed. The copyright holder has made the manuscript available under a Creative Commons Attribution 4.0 International (CC BY) license and consented to have it forwarded to EarthArXiv for public posting.

Table 5: Predicted Short-Term Drought Events under the Future Climate of Wukro

Drought year	DD (months)	Inception	Termination	Tot. Magnitude	Mean Intensity
2054	5	Feb	Jun	-6.961778	-1.392356
2055	2	Jun	Jul	-2.853608	-1.426804
2056	2	Jan	Feb	-3.561939	-1.780970
2057	2	Nov	Dec	-2.188497	-1.094248
2058-2059	6	Aug	Jan	-7.467206	-1.244534
2059	4	Sep	Dec	-5.605437	-1.401359
2060	3	Sep	Nov	-4.217291	-1.405764
2061-2062	4	Nov	Feb	-5.828884	-1.457221
2062	3	Sep	Nov	-3.555122	-1.185041
2063	5	Jul	Nov	-6.693344	-1.338669
2064	4	Jul	Oct	-5.892976	-1.473244
2065	5	Jul	Nov	-6.886048	-1.377210
2066	3	Aug	Oct	-3.349437	-1.116479
2067-2068	4	Oct	Jan	-6.054706	-1.513676
2069	4	Mar	Jun	-8.890474	-2.222618
2084	5	Feb	Jun	-6.087338	-1.217468
2085	2	Jan	Feb	-2.679236	-1.339618
2085	2	Jun	Jul	-2.618877	-1.309439
2086	2	Jan	Feb	-3.449002	-1.724501
2088-2089	6	Aug	Jan	-7.681349	-1.280225
2089	4	Sep	Dec	-5.50935	-1.377338
2090	3	Sep	Nov	-4.070344	-1.356781
2091-2092	4	Nov	Feb	-5.994511	-1.498628

This manuscript is a preprint and has not been peer reviewed. The copyright holder has made the manuscript available under a Creative Commons Attribution 4.0 International (CC BY) license and consented to have it forwarded to EarthArXiv for public posting.

2092	3	Sep	Nov	-3.64322	-1.214407
2093	5	Jul	Nov	-6.378125	-1.275625
2094	5	Jul	Nov	-6.959671	-1.391934
2095	5	Jul	Nov	-6.721358	-1.344272
2096	3	Aug	Oct	-3.365769	-1.121923
2097-2098	3	Nov	Jan	-4.674672	-1.340074
2099	4	Mar	Jun	-7.462898	-1.865725

Table 6: Predicted Long Term Drought Events under the Future Climate of Wukro

Drought year	DD (months)	Inception	Termination	Tot. Magnitude	Mean Intensity
2055-2056	10	Aug	May	-11.86059	-1.186059
2057-2059	15	Nov	Jan	-23.63112	-1.575408
2061-2063	21	Jul	Mar	-26.00165	-1.242897
2064	5	Apr	Aug	-5.275951	-1.055190
2066	3	Feb	Apr	-3.041786	-1.013929
2066-2067	5	Nov	Mar	-5.277121	-1.055424
2067-2068	9	Nov	Jul	-11.93346	-1.325940
2082-2083	8	Aug	Mar	-1.07063	-0.133829
2084	4	Apr	Jul	-1.212696	-0.303174
2087-2088	8	Aug	Mar	-1.535345	-0.191918
2093-2094	8	Jun	Feb	-1.006743	-0.125843
2094-2096	24	Apr	Mar	-1.156088	-0.048170
2097	3	Apr	Jun	-1.18687	-0.395623
2097-2099	20	Dec	Jul	-1.657871	-0.082894

This manuscript is a preprint and has not been peer reviewed. The copyright holder has made the manuscript available under a Creative Commons Attribution 4.0 International (CC BY) license and consented to have it forwarded to EarthArXiv for public posting.

4 Discussion

The changing climate is intensifying drought worldwide, causing crop destruction, environmental damage, and economic losses worth billions of moneys (Danandeh et al., 2020). Drought analysis is therefore necessary as it helps understand, predict, and mitigate such impacts on agriculture, water resources, ecosystems, and economies. Understanding past and future drought characteristics (duration, magnitude and intensity) is pivotal to the planning of adaption measures to lessen the impacts of droughts (Vu et al., 2017).

Although drought occurs in various forms, empirical evidence identifies temperature and precipitation as the primary drivers of meteorological and agricultural drought (Yi Liu et al., 2023; Webb & Braun, 1990). Correspondingly, this study recorded an increase in mean daily temperature (T_{Mean}) and precipitation in the study area. Generally, an increase in minimum and maximum temperature has been reported in several scientific reports, including Lamaro et al (2023), Kidanu et al. (2009), IPCC (2007) and IPCC (2001). In the future, the increasing temperatures will likely cause an upsurge in the atmospheric evaporative demand, thereby increasing drought risks in drought-prone areas. Harmoniously with NAPA (2007), and IPCC (2007), a percentage increase in annual mean rainfall is predicted over the study area. Even though the three locations (stations) are not geographically far apart, Atsbi is likely to experience a greater increase in mean annual rainfall relative to Wukro and Fatsi. Such spatial variability was reported by Tafere et al (2019) and Hulme et al (2005) in their study of the Tigray and East African climate respectively. Additionally, Lamaro et al (2023), in their study on the impact of future climate on sweetpotato production in the Tigray region, reported that there would be an increase in precipitation though countered by an increase in temperature, which shall jeopardize crop yield in this locality because of increased evapotranspiration. An increase in mean daily temperature will increase potential evapotranspiration, affecting soil water balance, crop yield and general agricultural profitability.

Using historical climate data, the SPI and SPEI indices precisely identified the historical drought years corresponding to other empirical findings (NAPA, 2007a; NAPA, 2007b). According to NAPA (2007b),

This manuscript is a preprint and has not been peer reviewed. The copyright holder has made the manuscript available under a Creative Commons Attribution 4.0 International (CC BY) license and consented to have it forwarded to EarthArXiv for public posting.

drought years that affected Ethiopia were 1618, 1864-66, 1876-78, 1880, 1888-1892, 1899-1900, 1913-1914, 1920-1922, 1932-1934, 1953, 1957, 1958, 1964-1966, 1973-1974, 1982, 1983-1984, 1987-1988, 1990-1992, 1993-94, 1999, 2000 and 2002/2003. Our findings also agree with Viste et al. (2013) and NAPA (2007a), who reported that the years 1988-1992 were dry in the whole of Ethiopia, except for a small positive deviation in the Northeastern Rift Valley (I) in 1990. This study also observed the years 1990, 1997 and 2003 as Ethiopia's drought years. This is consistent with several authors (Adane et al., 2012; NAPA (16); Seleshi and Zanke (17). According to Seleshi and Zanke (2004), the year 1997 was the drought year that resulted in low agricultural production, which affected millions of rural poor farmers, pastoralists, domestic and wild animals, with serious degradation of the environment. For all three locations (stations), this study observed that the peak drought intensity over the past 30 years occurred at different times. This validates the fact that drought characteristics can vary spatially (Tafere et al., 2019; Wilhite and Glantz, 1985).

Although the predicted climate showed increased precipitation in the future, it's characteristically intermittent wet-dry cycles, coupled with higher evapotranspiration due to higher temperatures. Some years will receive below normal precipitation values; thus, drought remains an imminent threat under the future climate in the study area. Using the projected climate data of the study area, the SPI and SPEI indices revealed an increase in drought magnitude under the future climate of the study area. The projected increase in drought magnitude further proves that although precipitation is predicted to increase above the baseline under a future climate of the study area, temporal variability is imminent, as some years will experience deficits that will consequently lead to drought episodes. This finding is in agreement with similar authors who documented an increase in drought trend on all time scales with an average very short drought return period (Tafere et al., 2019). The IPCC's Sixth Assessment Report (AR6) (2021) also projected increased drought magnitude due to climate change, particularly in semi-arid and arid regions (Legg, 2021). The magnitude of drought in the future climate will likely be further worsened by the impact of rising temperatures on soil moisture balance (Sharma and Ravindranath, 2019). In the end-term, there seems to be

This manuscript is a preprint and has not been peer reviewed. The copyright holder has made the manuscript available under a Creative Commons Attribution 4.0 International (CC BY) license and consented to have it forwarded to EarthArXiv for public posting.

a slightly lower increase in drought magnitude. This could be attributed to the projected increase in precipitation in the end-term time segment. Meanwhile, for the predicted rise in drought magnitude under all-time segments and emission scenarios, the increase exhibited by SPEI-12 is superior to SPI-12. This could be because SPEI indices captured impacts of higher temperatures on atmospheric evaporative demand under the future climate. According to Thornton et al (2011), the most significant impact of an increase in drought magnitude is likely to be experienced negatively on agricultural production.

Our study also revealed an increase in drought duration under the future climate, though lopsidedly in the three study locations. The comparatively slightly higher drought duration (number of drought months) SPEI-12 timescale explained in all the three stations compared to SPI-12 could probably be attributed to the fact that including temperature in the meteorological indices (SPEI) increased its sensitivity for the identification of drought phenomena. The observed greater increase in the duration of long-term drought that shall be experienced during the end of the century, shown by both SPEI-12 and SPI-12, shall affect peoples' livelihood, especially for the vulnerable smallholder farmers. This finding resonates well with Tafera et al (2019) who recorded a statistically significant drought trend with varying duration, severity, intensity and frequency in Tigray region. According to Margaret (2003) and Thornton et al., (2011), an increase in drought duration under future climate may directly relate to an increase in the frequency of its occurrence and such a trend may result in to narrowing of livelihood options for marginalized community hence aggravating the already worse condition of their livelihood.

5 Conclusion

Drought has been one of the most damaging natural disasters to humanity in recent years. Coupled with climate change, drought events may cause more serious impacts than ever before. The analysis of the meteorological drought events under the past and future climate of the study area using SPI and SPEI indices revealed that the years 1982-83, 1984, 1985,1999, 2002, 2003, 2004, 2005, 2008 and 2009 were drought years in the study area. In the past, the magnitude of short-term drought was highest in Atsbi and

This manuscript is a preprint and has not been peer reviewed. The copyright holder has made the manuscript available under a Creative Commons Attribution 4.0 International (CC BY) license and consented to have it forwarded to EarthArXiv for public posting.

Wukro. For long-term drought, the magnitude was highest in Atsbi and Fatsi. The predicted climate of the study area showed a rise in average daily temperature in all the stations, but a higher upsurge is observed in Atsbi. Mean annual rainfall will also increase in the future, though with temporal variability. Using the predicted climate data, 4-months SPI/SPEI indices, Fatsi will experience a higher increase in short-term drought magnitude and an increase in severe drought events in the future than Atsbi and Wukro. Conversely, in the long-term drought, Atsbi and Wukro will experience a greater upsurge in total drought magnitude than Fatsi. For short-term drought events, Fatsi is likely to experience a significant increase in the total number of dry months, meanwhile, Wukro will experience an increase in the number of dry months in long-term drought, to Atsbi and Fatsi. In Atsbi, the frequency of severe drought is projected to increase both in short-term and long-term drought events. Regardless of the predicted increase in mean annual rainfall, some years will inevitably experience a deficit that will be tantamount to drought events coupled with higher evapotranspiration. Moreover, the predicted increase in precipitation under the future climate shall have uneven temporal characteristics/variability. There is, therefore, a need for improved soil and water conservation practices that minimize potential evapotranspiration. Additionally, rainwater harvesting that provides an auxiliary option for use when water is not available should be promoted. Adoption of other climate smart agriculture practices such as early maturing genotypes or cultivars would make crops escape droughts and yield for farmers.

Acknowledgements

This research was supported in part by the Transdisciplinary Training for Resource Efficiency and Climate Change Adaptation in Africa (TRECCAFRICA) and the African Climate Change Adaptation Initiative (ACCAI). The authors wish to thank Dr. Alexander C Ruane - NASA for providing AgMERRA Climate Forcing Datasets. Special thanks go to the entire Mekelle University – Institute of Climate and Society (MU-ICS) fraternity for their encouragement and unreserved support in conducting this study.

This manuscript is a preprint and has not been peer reviewed. The copyright holder has made the manuscript available under a Creative Commons Attribution 4.0 International (CC BY) license and consented to have it forwarded to EarthArXiv for public posting.

Author contribution: Conceptualization: DR, AG, AZ; investigation: DR, AG, AZ; formal analysis: DR, AG, AZ, writing DR, GPL, AG, AZ. All authors have read and agreed to the published version of the manuscript.

Data Availability: The raw data presented in this study are available on request from the corresponding author.

Declaration of interest

☐ The authors declare that they have no known competing financial interests or personal relationships that could have appeared to influence the work reported in this paper.

☒ The authors declare the following financial interests/personal relationships which may be considered as potential competing interests:

The authors acknowledge support from Transdisciplinary Training Resource Efficiency and Climate Change Adaptation in Africa (TRECCAFRICA), the African Climate Change Adaptation Initiative (ACCAI). Damasco Rubangakene also reports a relationship with the African Climate Change Adaptation Initiative (ACCAI) and DANIDA VUCCA (Vulnerability and Climate Change Adaptation and in Conflict-Affected Regions, Grant number 23-09-KU.

References

Abramowitz M, Stegun IA. Handbook of Mathematical Functions Dover Publications. New York. 1965;361.

This manuscript is a preprint and has not been peer reviewed. The copyright holder has made the manuscript available under a Creative Commons Attribution 4.0 International (CC BY) license and consented to have it forwarded to EarthArXiv for public posting.

Adane T, Alemu M, Zenebe G, & Assefa S. Climate Conventions and Africa/Ethiopia: EDRI Research Report 15. Ethiopian Development Research Institute, Addis Ababa: Ethiopian Development Research Institute, 2012.

Adib A, Haidari B, Lotfirad M, Sasani H. Evaluating climatic change effects on EC and runoff in the near future (2020–2059) and far future (2060–2099) in arid and semi-arid watersheds. Applied Water Science. 2023; 13(6):122.

Asheber S. Mitigating Drought: Policy Impact Evaluation A Case of Tigray Region , Ethiopia Mitigating Drought : Policy Impact Evaluation A Case of Tigray Region , Ethiopia. MSc Thesis submitted to the Faculty of Geo-information and Earth Observation, University of Twente, Netherlands, 2010; 89.

Asseng S, Cammarano D, Basso B, Chung U, Alderman PD, Sonder K, Reynolds M, Lobell DB. Hot spots of wheat yield decline with rising temperatures. Global Change Biology. 2016 Nov 10;23(6):2464-72.

Conway G. The science of climate change in Africa: impacts and adaptation. Grantham institute for climate change discussion paper. 2009;1:24.

Cottrell RS, Nash KL, Halpern BS, Remenyi TA, Corney SP, Fleming A, Fulton EA, Hornborg S, Johne A, Watson RA, Blanchard JL. Food production shocks across land and sea. Nature Sustainability. 2019; 2(2):130-7.

This manuscript is a preprint and has not been peer reviewed. The copyright holder has made the manuscript available under a Creative Commons Attribution 4.0 International (CC BY) license and consented to have it forwarded to EarthArXiv for public posting.

Danandeh Mehr A, Sorman AU, Kahya E, Hesami Afshar M. Climate change impacts on meteorological drought using SPI and SPEI: case study of Ankara, Turkey. Hydrological Sciences Journal. 2020; 65(2):254-68.

Devereux S, Sussex I. Food insecurity in Ethiopia. Brighton: Institute for Development Studies; 2000 Oct.

Doesken NJ, McKee TB, Kleist J. Development of a surface water supply index for the western United States. Climatology Report 91.1991.

Edwards DC, McKee TB. Characteristics of 20th century drought in the United States at multiple timescales, Colorado State University: Fort Collins. Climatology Report, 97. 1997.

Etsay H, Oniki S, Berhe M, Negash T. The watershed communal land management and livelihood of rural households in Kilte Awlaelo Woreda, Tigray region, Ethiopia. Sustainability. 2022; 14(20):13676.

FAO World Food and Agriculture. FAO Statistical Yearbook Series. 2012. *URL:* https://books.google.co.ug/books/download/Fao_Statistical_Yearbook_2012.bibtex?id=DBfOuQAACAAJ&output=bibtex

Gebrehiwot T, Van der Veen A, Maathuis B. Spatial and temporal assessment of drought in the Northern highlands of Ethiopia. International Journal of Applied Earth Observation and Geoinformation. 2011; 13(3):309-21.

This manuscript is a preprint and has not been peer reviewed. The copyright holder has made the manuscript available under a Creative Commons Attribution 4.0 International (CC BY) license and consented to have it forwarded to EarthArXiv for public posting.

Gebrekiros G, Araya A, Yemane T. Modeling impact of climate change and variability on sorghum production in southern zone of Tigray, Ethiopia. 2016; 322

Ghaleb F, Mario M, Sandra AN. Regional landsat-based drought monitoring from 1982 to 2014. Climate. 2015; 3(3):563-77.

Guttman NB. Accepting the standardized precipitation index: a calculation algorithm 1. JAWRA Journal of the American Water Resources Association. 1999; 35(2):311-22.

Hargreaves G H. Accuracy of estimated reference evapotranspiration J. Irrig. Drain. Eng. ASCE, 1989.

He X, Estes L, Konar M, Tian D, Anghileri D, Baylis K, Evans TP, Sheffield J. Integrated approaches to understanding and reducing drought impact on food security across scales. Current Opinion in Environmental Sustainability. 2019; 40:43-54.

Hudson N, Ruane A. Guide for running AgMIP climate scenario generation tools with R. AgMIP. Available online: http://www. agmip. org/wp-content/uploads/2013/10/Guide-for-Running-AgMIPClimate-Scenario-Generation-with. 2013.

Hulme M, Doherty R, Ngara T, New MG, Low PS. Global warming and African climate change: a reassessment. InClimate Change and Africa 2005 (pp. 29-40).

IPCC. Climate Change 2007: Impacts, Adaptation and Vulnerability. Contribution of Working Group II to the Fourth Assessment Report of the Intergovernmental Panel on Climate Change.

Ipcc A. Ipcc fifth assessment report—synthesis report. IPPC Rome, Italy. 2014; 450.

This manuscript is a preprint and has not been peer reviewed. The copyright holder has made the manuscript available under a Creative Commons Attribution 4.0 International (CC BY) license and consented to have it forwarded to EarthArXiv for public posting.

Terra K, Van Rompaey A, Poesen J, Welday Y, Deckers J. Impact of climate change on small-holder farming: A case of Eastern Tigray, Northern Ethiopia. African Crop Science Journal. 2012; 20:337-47.

Kidanu A, Rovin K, Hardee-Cleaveland K. Linking population, fertility and family planning with adaptation to climate change: views from Ethiopia. Washington, DC, USA: Population Action International; 2009 Oct.

Kumar MN, Murthy CS, Sai MV, Roy PS. On the use of Standardized Precipitation Index (SPI) for drought intensity assessment. Meteorol. Appl., 2009; 16: 381-389.

Lamaro GP, Tsehaye Y, Girma A, Rubangakene D. The impact of future climate on orange-fleshed sweet potato production in arid areas of Northern Ethiopia. A case study in Afar region. Heliyon. 2023; 9(7).

Lee SH, Yoo SH, Choi JY, Bae S. Assessment of the impact of climate change on drought characteristics in the Hwanghae Plain, North Korea using time series SPI and SPEI: 1981–2100. Water. 2017; 9(8):579.

Legg S. IPCC, 2021: Climate change 2021-the physical science basis. Interaction. 2021; 49(4):44-5.

Manaye A, Afewerk A, Manjur B, Solomon N. The Effect of the war on smallholder agriculture in Tigray, Northern Ethiopia. Cogent Food & Agriculture. 2023; 9(1):2247696.

Margaret F. Planning for the Next Drought: Ethiopia Case Study USAID, Washington. 2003: 100-200.

This manuscript is a preprint and has not been peer reviewed. The copyright holder has made the manuscript available under a Creative Commons Attribution 4.0 International (CC BY) license and consented to have it forwarded to EarthArXiv for public posting.

McKee TB, Doesken NJ, Kleist J. The relationship of drought frequency and duration to time scales. InProceedings of the 8th Conference on Applied Climatology 1993 Jan 17 (Vol. 17, No. 22, pp. 179-183).

NAPA. Climate change national adaptation programme of action (Napa) of Ethiopia. National Meteorological Services Agency, Ministry of Water Resources, Federal Democratic Republic of Ethiopia, Addis Ababa. 2007 Jun.

NAPA. Climate change National Adaptation Programme of Action (NAPA) of Ethiopia, National Meteorological Agency, Addis Ababa, Ethiopia.2007a

NAPA. Climate Change National Adaptation Programme of Action (Napa) Of Ethiopia. In: Tadege, A. (Ed.). Addis Ababa, Ethiopia: National Meteorological Agency. 2007b

Nasir J, Assefa E, Zeleke T, Gidey E. Meteorological Drought in Northwestern Escarpment of Ethiopian Rift Valley: detection seasonal and spatial trends. Environmental Systems Research. 2021; 10(1):16.

Orimoloye IR. Agricultural drought and its potential impacts: enabling decision-support for food security in vulnerable regions. Frontiers in Sustainable Food Systems. 2022; 6:838824.

Otim D. Drought Analysis for Busia District (Uganda), Istituto Agronomico per l'Oltremare, Facoltá di Agraria. Università degli Studi di Firenze, Florence. 2008.

Patel NR, Chopra P, Dadhwal VK. Analyzing spatial patterns of meteorological drought using standardized precipitation index. Meteorological Applications: A journal of forecasting, practical applications, training techniques and modelling. 2007; 14(4):329-36.

This manuscript is a preprint and has not been peer reviewed. The copyright holder has made the manuscript available under a Creative Commons Attribution 4.0 International (CC BY) license and consented to have it forwarded to EarthArXiv for public posting.

R-Core-Team R. A language and environment for statistical computing. R Foundation for Statistical Computing, Vienna, Austria. 2017.

Rojas O, Racionzer IP, Li Y. Surveillance of agricultural drought worldwide from space using the FAO-Agriculture Stress Index System (ASIS). 2019 edition of the Global Assessment Report on Disaster Risk Reduction; 2019.

Rubangakene D. Modeling the potential impact of future climate on barley (Hordeum vulgare L.) productivity and analysis of past and future meteorological and agricultural drought in the Eastern Tigray, Northern Ethiopia. A Thesis Submitted to the Institute of Climate and Society in Partial Fulfillment for the Award of Master of Science in Climate and Society: Climate Science Specialization of Mekelle University. 2018.

Seleshi Y, Zanke U. Recent changes in rainfall and rainy days in Ethiopia. International Journal of Climatology: A Journal of the Royal Meteorological Society. 2004; 24(8):973-83.

Sharma J, Ravindranath NH. Applying IPCC 2014 framework for hazard-specific vulnerability assessment under climate change. Environmental Research Communications. 2019; 1(5):051004.

Tefera AS, Ayoade JO, Bello NJ. Comparative analyses of SPI and SPEI as drought assessment tools in Tigray Region, Northern Ethiopia. SN Applied Sciences. 2019; 1(10):1265.

Thom HC. A note on the gamma distribution. Monthly weather review. 1958; 86(4):117-22.

This manuscript is a preprint and has not been peer reviewed. The copyright holder has made the manuscript available under a Creative Commons Attribution 4.0 International (CC BY) license and consented to have it forwarded to EarthArXiv for public posting.

Thornton PK, Jones PG, Ericksen PJ, Challinor AJ. Agriculture and food systems in sub-Saharan Africa in a 4 C+ world. Philosophical transactions of the royal Society A: Mathematical, physical and engineering sciences. 2011; 369(1934):117-36.

Vicente-Serrano SM, Beguería S, López-Moreno JI. A multiscalar drought index sensitive to global warming: the standardized precipitation evapotranspiration index. Journal of climate. 2010; 23(7):1696-718.

Viste E, Korecha D, Sorteberg A. Recent drought and precipitation tendencies in Ethiopia. Theoretical and Applied Climatology. 2013; 112(3):535-51.

Vu MT, Vo ND, Gourbesville P, Raghavan SV, Liong SY. Hydro-meteorological drought assessment under climate change impact over the Vu Gia–Thu Bon river basin, Vietnam. Hydrological Sciences Journal. 2017; 62(10):1654-68.

Webb P, Van Braun J. Drought and food shortages in Ethiopia. A preliminary review of effects and policy implications. IFPRI, Washington DC. 1990.

Wilcke RA, Bärring L. Selecting regional climate scenarios for impact modelling studies. Environmental Modelling & Software. 2016; 78:191-201.

Wilhite DA, Glantz MH. Understanding: the drought phenomenon: the role of definitions. Water international. 1985 Jan 1;10(3):111-20.

World Meteorological Organization (WMO). Standardized precipitation index user guide. J. Appl. Bacteriol.. 2012; 63(3):197-200.

Gan G, Ma C, Wu J. Data Clustering: Theory, Algorithms, and Applications. SIAM; 2007

This manuscript is a preprint and has not been peer reviewed. The copyright holder has made the manuscript available under a Creative Commons Attribution 4.0 International (CC BY) license and consented to have it forwarded to EarthArXiv for public posting.

Liu Y, Yuan S, Zhu Y, Ren L, Chen R, Zhu X, Xia R. The patterns, magnitude, and drivers of unprecedented 2022 mega-drought in the Yangtze River Basin, China. Environmental Research Letters. 2023; 18(11):114006.

1. . !!! INVALID CITATION !!! (Ghaleb et al., 2015; Thornton et al., 2011).
2. Gebrehiwot T, van der Veen A, Maathuis B. Spatial and temporal assessment of drought in the Northern highlands of Ethiopia. International Journal of Applied Earth Observation and Geoinformation. 2011;13(3):309-21.
3. Patel NR, Chopra P, Dadhwala VK. Analyzing spatial patterns of meteorological drought using Standardized precipitation index. Meteorological Application. 2007(14):329-36.
4. WMO. Standardized Precipitation Index User Guide (WMO-No1090), Geneva. 2012.
5. Kumar MN, Murthy CS, Saib MVRS, Royb PS. On the use of Standardized Precipitation Index (SPI) for drought intensity assessment. Meteorol Appl 2009;16 381-9 (2009).
6. Guttman NB. Accepting the Standardized Precipitation Index: a calculation algorithm. Journal of the American Water Resources Association. 1999;35:311-22.
7. Wu J, Gan G, Ma C. Data Clustering: Theory, Algorithms, and Applications. 2007:397-466. .
8. Thom HCS. A note on the gamma distribution, Monthly Weather 1958;Rev. 86 117-22.
9. Edwards DC, McKee TB. Characteristics of 20th century drought in the United States at multiple timescales, Colorado State University: Fort Collins. . Climatology Report. 1997;97(2).
10. Abramowitz M, Stegun IA. Handbook of Mathematical Formulas, Graphs, and Mathematical Tables. Dover Publications: New York. 1965.
11. Vicente-Serrano SM, Begueria S, Lopez-Moreno JI. A multi-scalar drought index sensitive to global warming. the Standardized Precipitation Evapotranspiration Index. 2010.
12. McKee TB, Doesken NJ, Kleist J. The Relationship of Drought Frequency and Duration to Time Scales. . Proceedings of the 8th Conference on Applied Climatology. 1993:17-22
13. . !!! INVALID CITATION !!! (Kassa et al., 2012).
14. Otim D. DROUGHT ANALYSIS FOR BUSIA DISTRICT (UGANDA): Florentina Studiorum 2008.
15. R-Core-Team. R: A language and environment for statistical computing. R Foundation for Statistical Computing, Vienna, Austria. 2017.
16. NAPA. Climate change National Adaptation Programme of Action (NAPA) of Ethiopia, National Meteorological Agency, Addis Ababa, Ethiopia. 2007.
17. Seleshi, Zanke U. RECENT CHANGES IN RAINFALL AND RAINY DAYS IN ETHIOPIA. INTERNATIONAL JOURNAL OF CLIMATOLOGY. 2004;24:973–83 (2004).